Supplementary Information

Itaconate-based nanoparticles induce immunometabolic reprogramming in macrophages and alleviate diet-induced obesity

Andrea L. Cottingham[1], Neda Mohaghegh[5], Sara M. Kolhatkar[1], Fanny Xu[1], Shruti Dharmaraj[1], Jacob R. Shaw[1], Sanmoy Pathak[6], Victor Andrade[1], Yan Shu[1], Abhinav P. Acharya[6], Alireza Hassani Najafabadi[4,5,7], Ryan M. Pearson[1,2,3,7]

1. Department of Pharmaceutical Sciences, University of Maryland School of Pharmacy, 20 N. Pine Street, Baltimore, MD 21201, US

2. Department of Microbiology and Immunology, University of Maryland School of Medicine, 685 W. Baltimore Street, Baltimore, MD 21201, US

3. Marlene and Stewart Greenebaum Comprehensive Cancer Center, University of Maryland School of Medicine, 22 S. Greene Street, Baltimore, MD 21201, US

4. Department of Pharmaceutical Sciences, University of Cincinnati James L. Winkle College of Pharmacy, Cincinnati, OH 45221 USA

5. Terasaki Institute for Biomedical Innovation, Los Angeles, CA 91367 USA

6. Case Western Reserve University, Cleveland, OH 44106 USA

7. Co-corresponding authors

Address correspondence to:
Ryan M. Pearson, Ph.D.
Associate Professor, Department of Pharmaceutical Sciences
Director, Bio- and Nanotechnology Center
University of Maryland School of Pharmacy
20 N. Pine Street
N525 Pharmacy Hall
Baltimore, MD 21201, USA
Phone: 410-706-3257
Email: rpearson@rx.umaryland.edu

Alireza Hassani Najafabadi, Ph.D.
Associate Professor, Department of Pharmaceutical Sciences
University of Cincinnati James L. Winkle College of Pharmacy
Cincinnati, OH 45221
Email: hassanaz@ucmail.uc.edu

KEYWORDS: Macrophage polarization, Inflammation, Obesity, Metabolism, Nanoparticle, Adipose tissue, Thermogenesis, Mitochondria

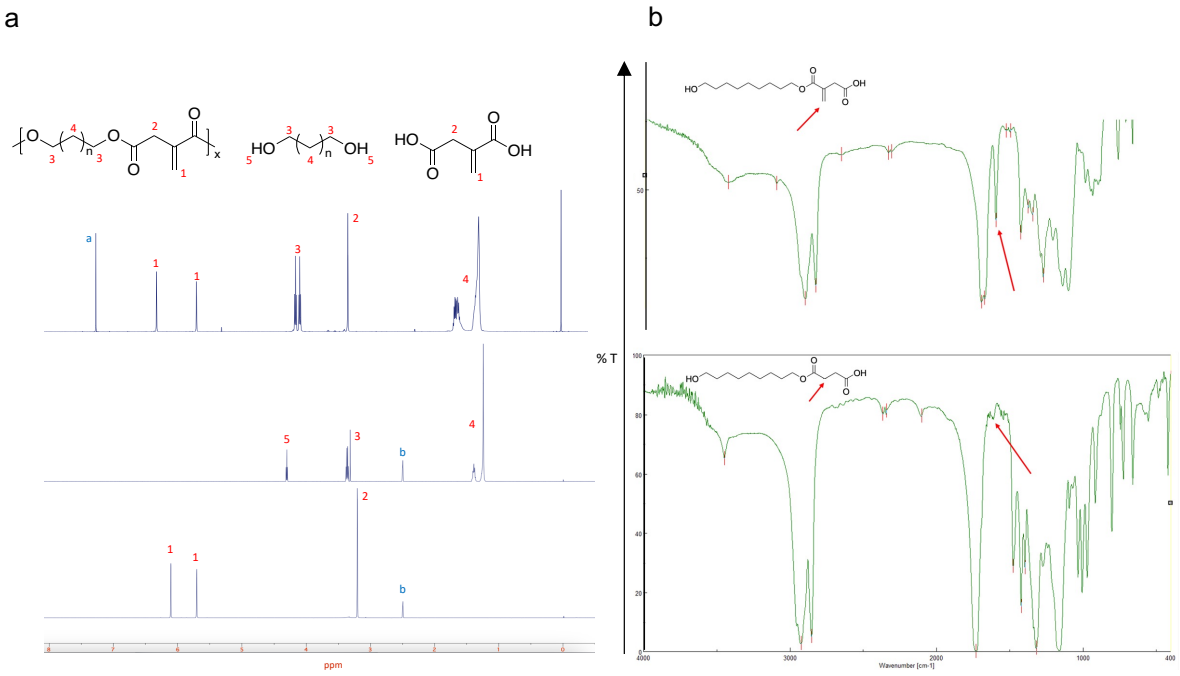

Supplementary Figure 1. Characterization via NMR and FTIR of pITA-C10. (a) ^{1}H-NMR spectrum of pITA-C10, 1,10-decandiol, and itaconic acid calibrated to TMS peak at 0.0 ppm. Numbers corresponding to matching protons across the spectras, with 'a' labeling the chloroform peak, and 'b' labeling the DMSO peak. **(b)** FTIR spectrum of pITA-C10 and poly(succinate)-C10. Red arrows are pointing to the vinylidene alkene at 1640 cm^{-1}, which is present in itaconate- but not succinate-containing polymers.

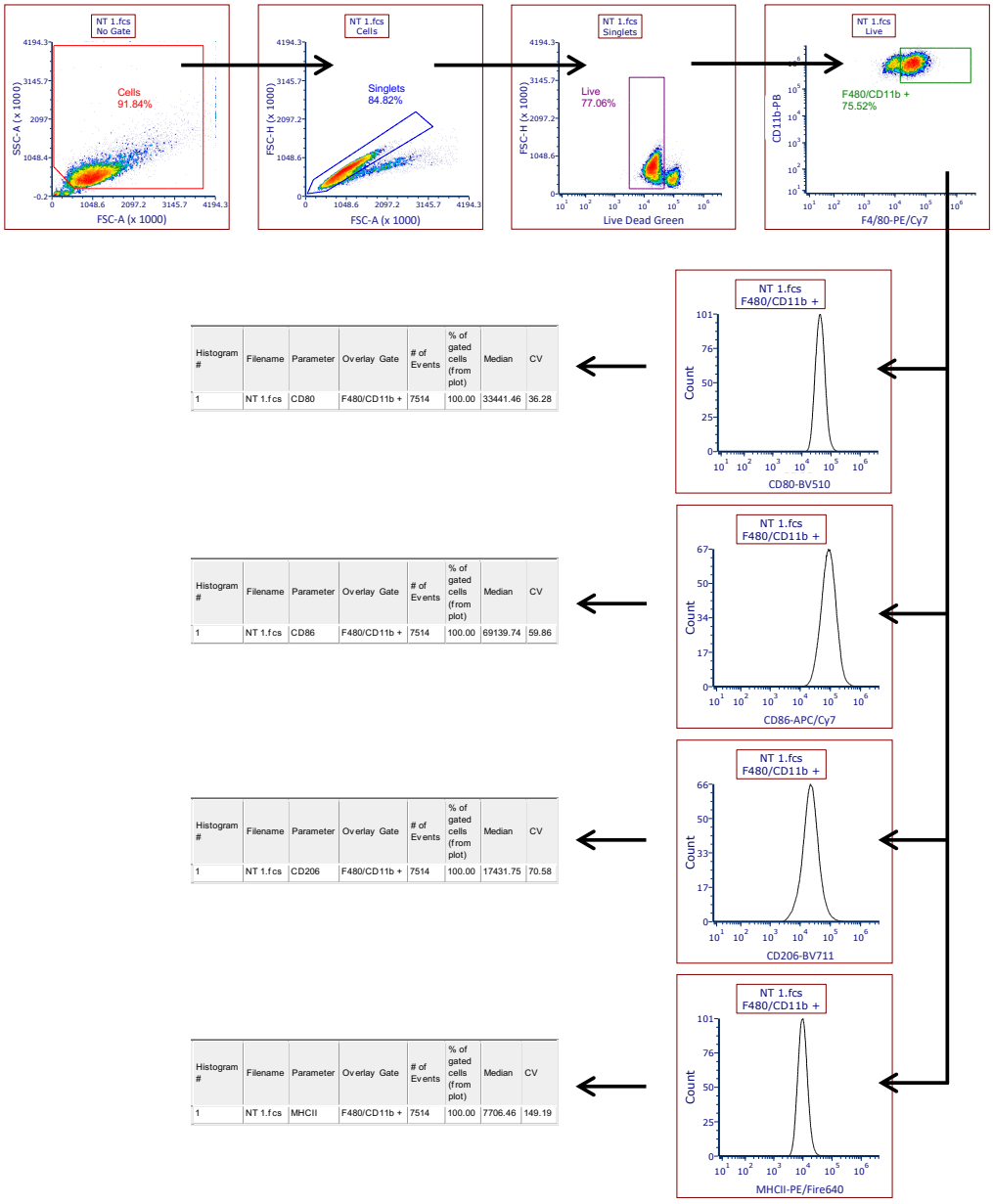

Supplementary Figure 2. Representative gating strategy for *in vitro* studies. Macrophages were analyzed on a Cytek Aurora 3 flow cytometer and gated as shown. The median value of the histogram was used as the MFI for data presentation.

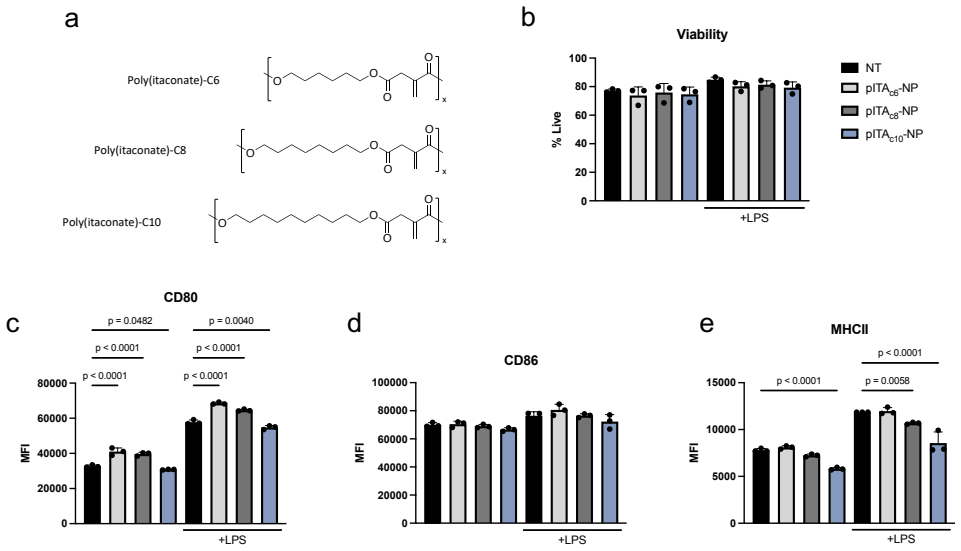

Supplementary Figure 3. Effect of pITA-NP formulations on macrophage viability and phenotypes. Itaconate-based polymers with various carbon chain length linkers **(a)** were formulated into nanoparticles and used to treat primary macrophages with and without prior LPS stimulation (100 ng/mL) for M1 macrophage induction. Using flow cytometry, the viability **(b)** as well as the surface expression of CD80 **(c)**, CD86 **(d)**, and MHCII **(e)**, represented by their mean fluorescence intensity (MFI), were evaluated 3 hours after NP treatment. Data is presented as mean values ± SD with $n = 3$ replicates per condition. Statistical differences were determined by one-way ANOVA with Fisher's LSD test, with p values listed above the compared groups.

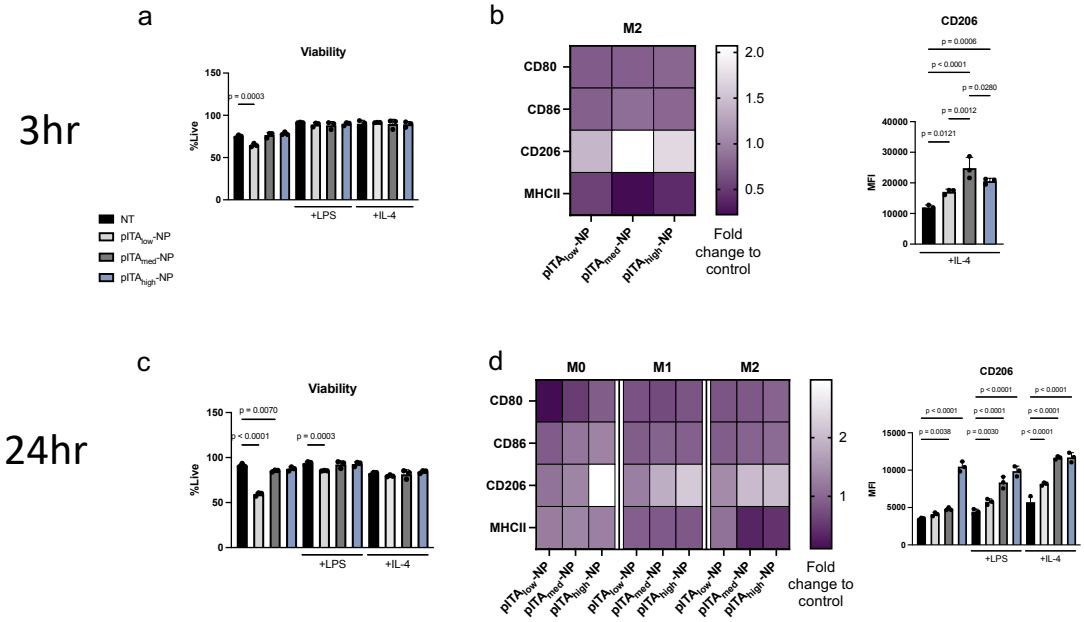

Supplementary Figure 4. Effect of pITA-C10 molecular weights on macrophage viability and phenotypes. ITA$_{C10}$ polymers were synthesized with three different molecular weights, low, medium, and high, then formulated into nanoparticles. Macrophages were stimulated overnight with LPS (100 ng/mL) or IL-4 (10 ng/mL) overnight to induce M1 and M2 phenotypes respectively. M0/M1/M2 macrophage viability was assessed 3 **(a)** and 24 hours **(c)** after 30 μg/mL NP treatment. Additionally, flow cytometry mean fluorescence intensity (MFI) of macrophage surface markers CD80, CD86, CD206, and MHCII was evaluated at 3 **(b)** and 24 hours **(d)**. Heat map data is presented as the mean fold change in MFI to the respective cell type control. Bar graphs are presented as mean MFI values ± SD, where *n* = 3 replicates per condition. Statistical differences were determined by one-way ANOVA with Fisher's LSD test, with p values listed above the compared groups.

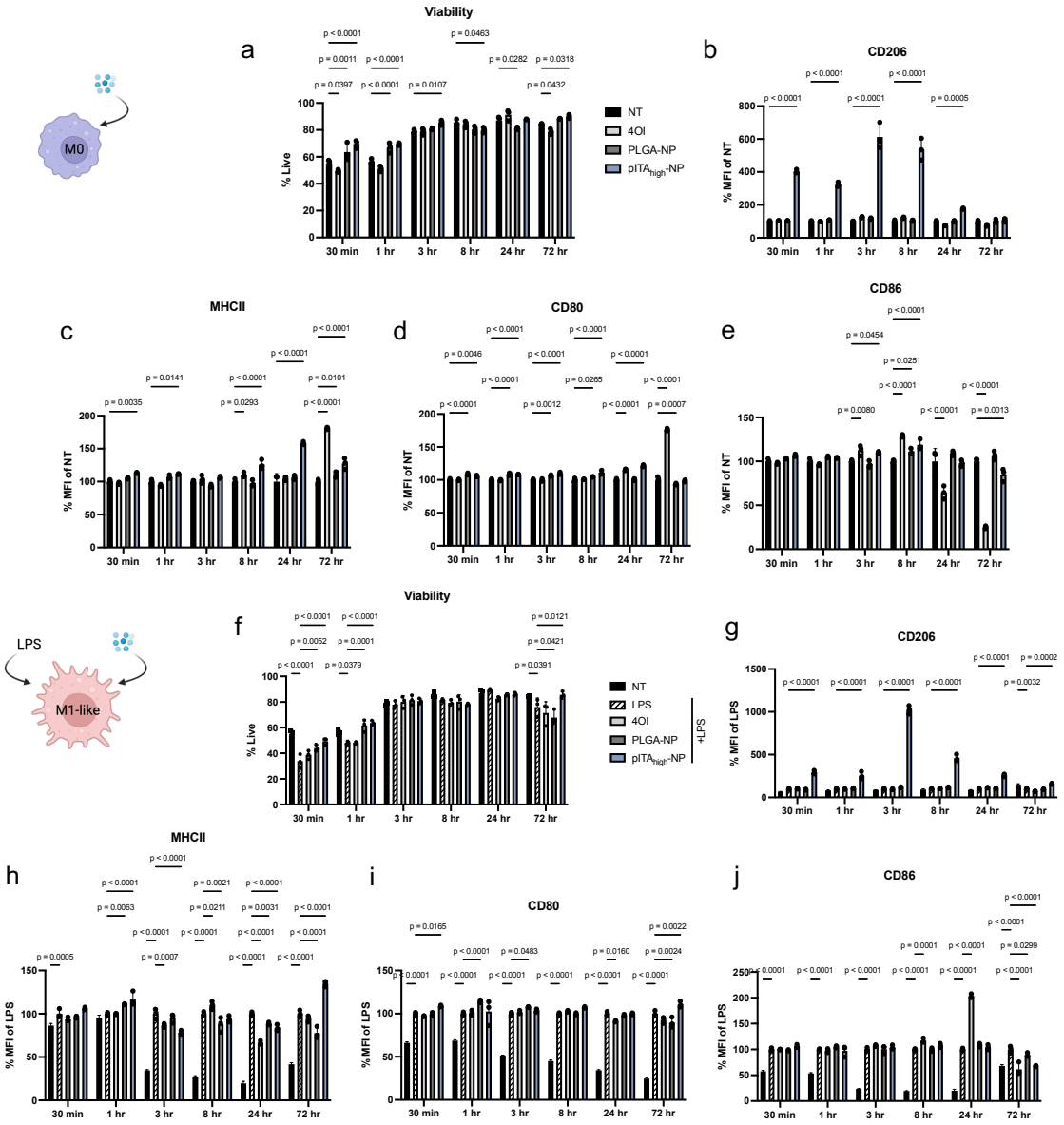

Supplementary Figure 5. Time dependent effects on polarization. To assess the phenotypic changes induced by NPs over time, M0 and M1 macrophages were treated with 30 μg/mL of Cy5.5 labeled NPs then at various timepoints, were collected and stained for key polarization surface markers. Viability of M0 **(a)** and M1 **(f)** macrophages was evaluated over 72 hours when treated with the membrane permeable ITA derivative, 4OI (125 μM) and PLGA and pITA$_{high}$-NPs (30 μg/mL). Additionally, flow cytometry mean fluorescence intensity (MFI) of macrophage surface markers CD206, MHCII, CD80, and CD86 was measured over 72 hours in both M0 **(b-e)** and M1 **(g-j)** conditions. Bar graphs are presented as mean MFI values ± SD, where *n* = 3 replicates per condition. Statistical differences were determined by two-way ANOVA with Tukey's multiple comparisons test, with p values listed above the compared groups.

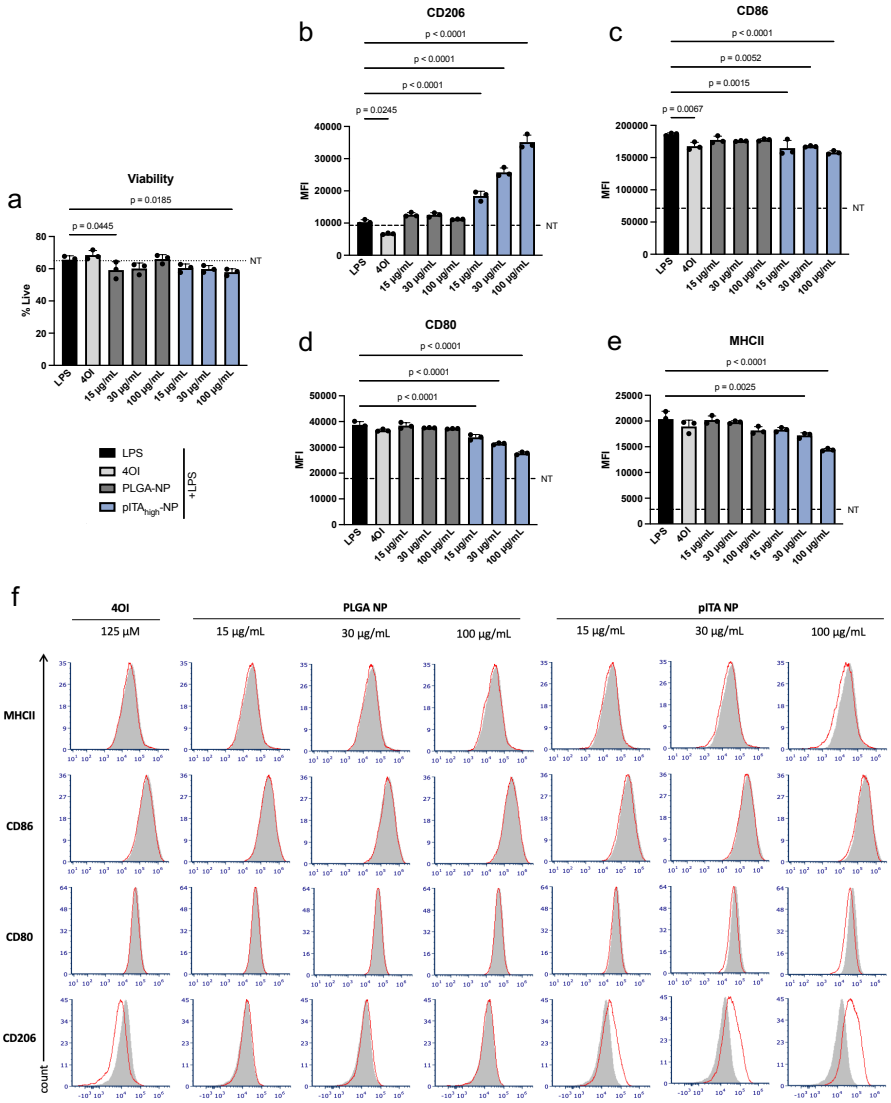

Supplementary Figure 6. Concentration-dependent effects on polarization. M1 polarized macrophages were treated with 3 different concentrations of pITA$_{high}$-NPs for 3 hours, and their viability was assessed **(a)**. The surface expression of CD206 **(b)**, CD86 **(c)**, CD80 **(d)**, and MHCII **(e)** was also evaluated using flow cytometry and reported using mean fluorescent intensity (MFI) represented by bar graphs. Dashed lines represent the M0 no treatment control MFI. Additionally, the surface marker expression was graphed as histograms, show live, F4/80+ and CD11b+ cell surface molecule expression with the red line histograms representing the treatment groups while the grey filled histograms represent the untreated LPS stimulated BMMØs **(f)**. *n* = 3 replicates per condition, and bar graphs are presented as mean MFI values ± SD. Statistical differences were determined by one-way ANOVA with Tukey's multiple comparisons test. P values listed above the compared groups.

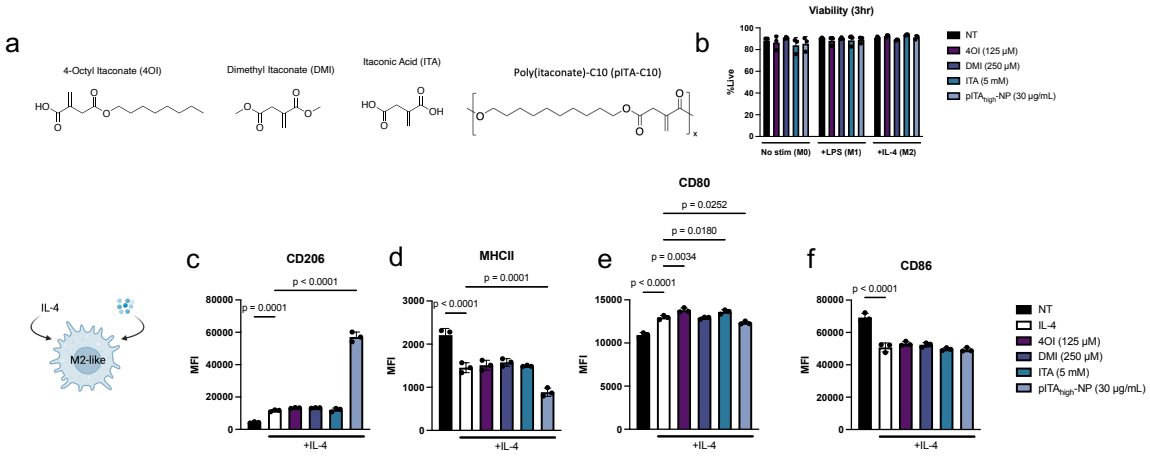

Supplementary Figure 7. pITA$_{high}$-NP and soluble controls elicit different effects at 3 hours in M2 macrophages. pITA$_{high}$-NPs were compared head-to-head to soluble derivatives **(a)**. M0/M1/M2-likemacrophages were induced then treated for 3 hours with 4OI (125 μM), DMI (250 (μM), ITA (5 mM) or pITA$_{high}$-NPs (30 μg/mL). Flow cytometry was then used to assess the viability **(b)** shown as % live, *n* =3. No significance between any group using two-way ANOVA with uncorrected Fisher's LSD test. Surface expression of CD206 **(c)**, MHCII **(d)**, CD80 **(e)**, and CD86 **(f)**, depicted as mean fluorescence intensity (MFI) ± SD with *n* = 3, was also evaluated in M2 (IL-4 stimulated) macrophages. Statistical differences were determined by one-way ANOVA with Dunnett's multiple comparisons test, with a single pooled variance. P values listed above the compared groups.

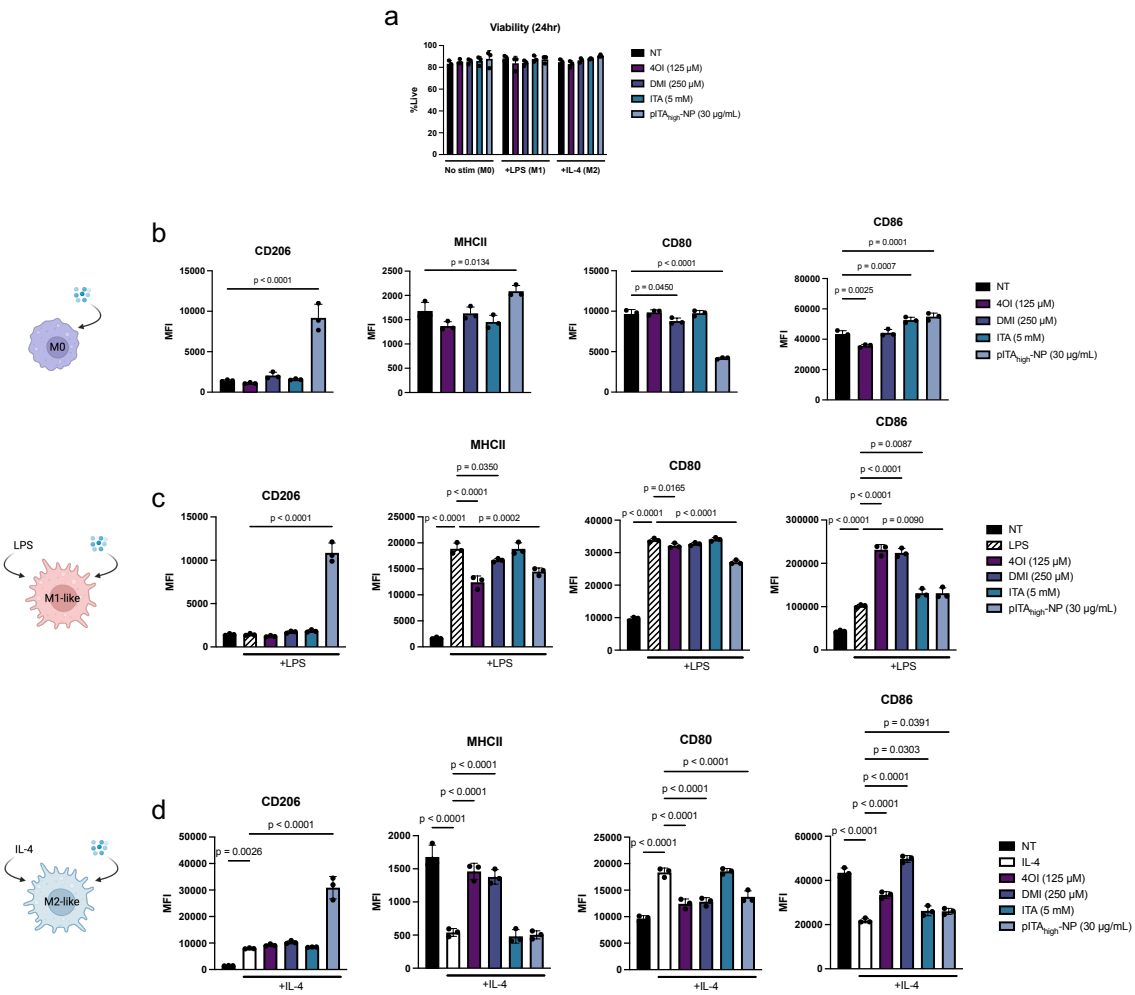

Supplementary Figure 8. pITA$_{high}$-NP and soluble controls elicit different effects at 24 hours in primary macrophages. Soluble and membrane permeable derivatives of itaconate were compared to pITA$_{high}$-NPs *in vitro*. Primary macrophages were pre-stimulated with LPS (100 ng/mL) or IL-4 (10 ng/mL) overnight where noted to induce M1 and M2 phenotypes respectively, then treated with 4OI (125 μM), DMI (250 μM), ITA (5 mM) or pITA$_{high}$-NPs (30 μg/mL) for 24 hours. Flow cytometry was then used to assess the viability **(a)** shown as % live, $n = 3$ for each condition. No significance between any group using two-way ANOVA with uncorrected Fisher's LSD test. Depicted as mean fluorescence intensity (MFI) of the surface expression of CD206, MHCII, CD80, and CD86 was measure in M0 (**b**), M1 (**c**), and M2 (**d**) macrophages after 24 hours of treatment. Bar graphs are presented as mean MFI values ± SD, where $n = 3$ for each condition. Statistical differences were determined by one-way ANOVA with Dunnett's multiple comparisons test, with a single pooled variance. P values listed above the compared groups.

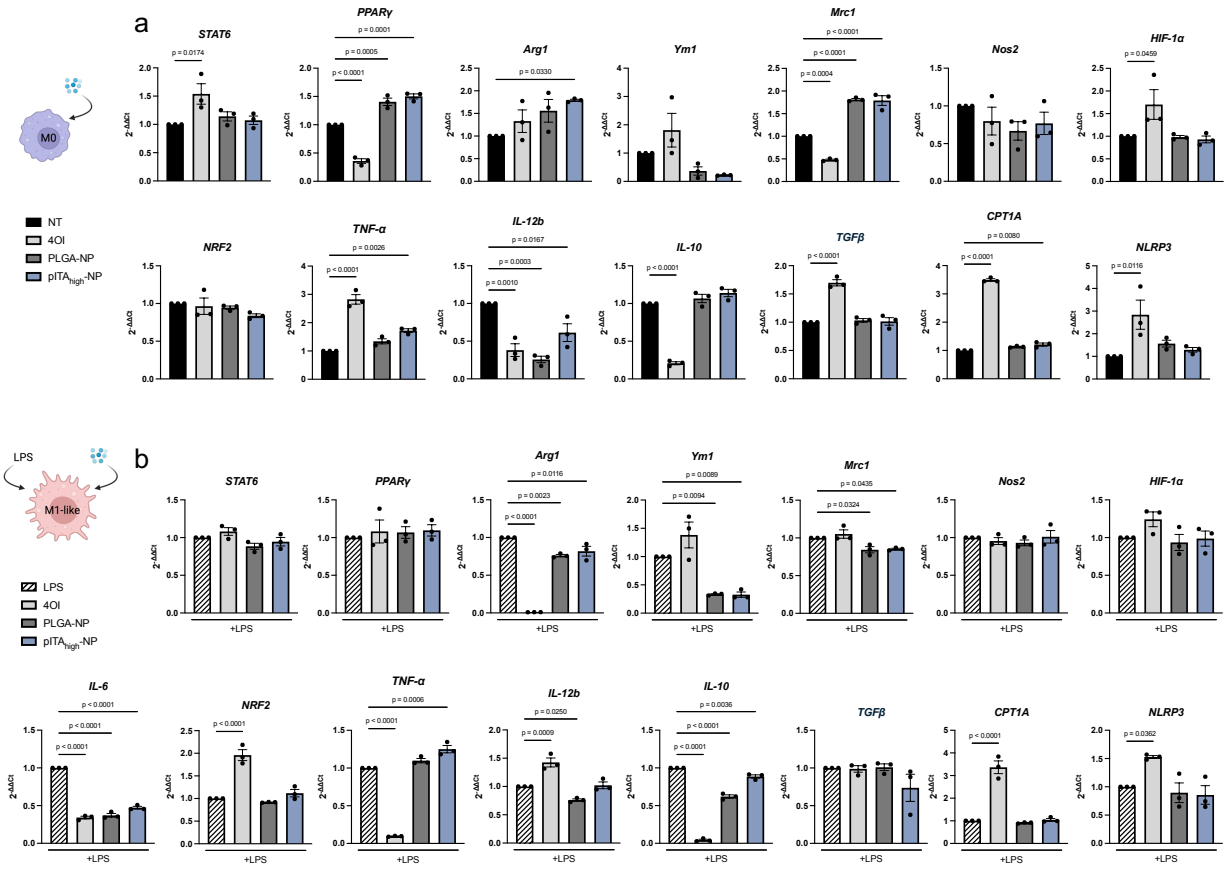

Supplementary Figure 9. Transcriptional changes induced by pITA$_{high}$-NPs. M0 and M1-like (100 ng/mL LPS stimmed overnight) macrophages were treated with 125 μM 4OI, or 30 μg/mL NPs for 24 hours, and RNA was collected and qPCR performed. *Stat6, Pparg, Arg1, Ym1, Mrc1, Nos2, Hif1α, Nrf2, Il6, Tnfa, Il12b, Il10, Tgfb, Cpt1a,* and *Nlrp3* were all evaluated, and normalized to no treatment in M0 macrophages **(a)** and LPS no treatment macrophages **(b)**. Bar graphs are representing $2^{-\Delta\Delta Ct}$ values in triplicate. Error reported as ± SEM. Statistical differences were determined by one-way ANOVA with Dunnett's multiple comparisons test, with a single pooled variance. P values listed above the compared groups.

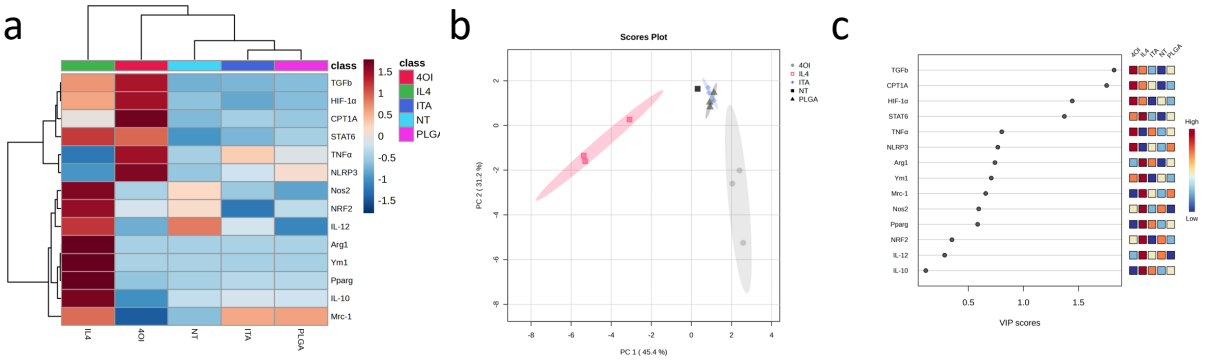

Supplementary Figure 10. plTA$_{high}$-NP treated macrophages display unique gene profiles compared to IL-4-induced M2-like macrophages. M0 macrophages were treated with 125 μM 4OI, or 30 μg/mL NPs for 24 hours. M2-like macrophages were generated by overnight 10 ng/mL IL-4 stimulation. Following treatment, RNA was collected and qPCR performed. Hierarchical clustering heatmaps (**a**), PCA plot (**b**), and VIP score plot (**c**) were generated using the $2^{-\Delta\Delta Ct}$ values in triplicate.

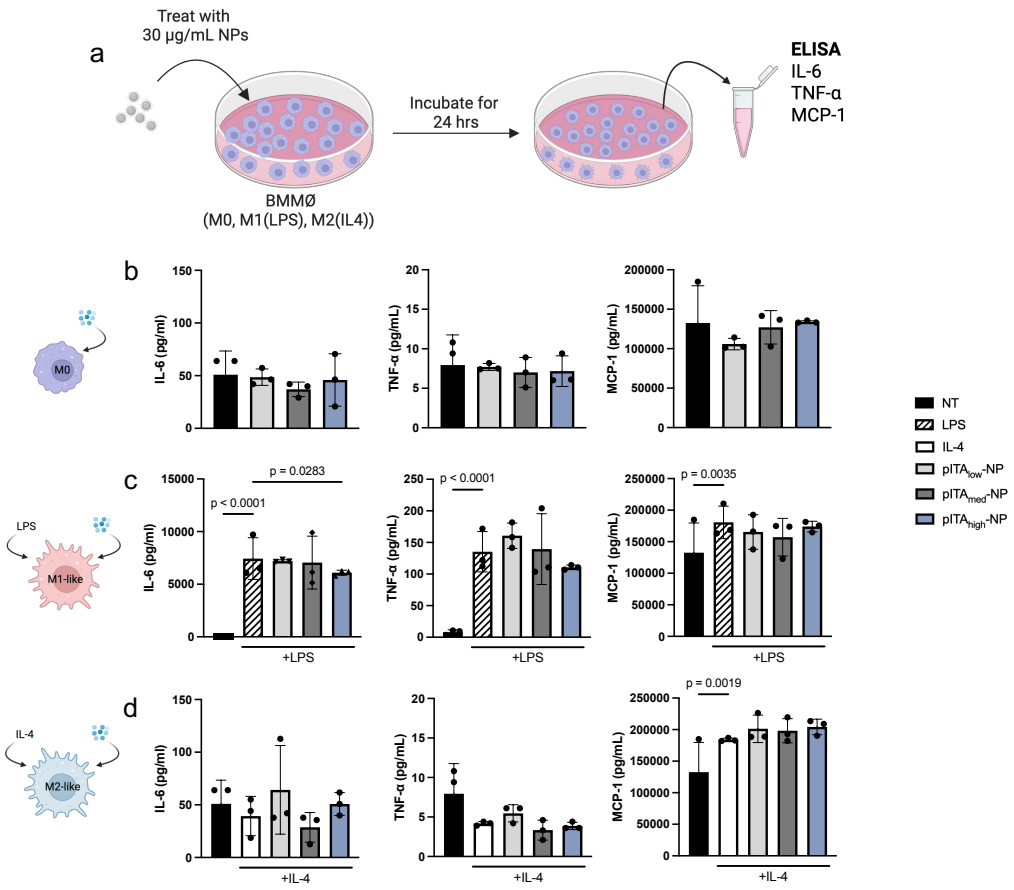

Supplementary Figure 11. Impact of polymer Mw on cytokine production. Macrophages were stimulated with LPS (100 ng/mL) or IL-4 (10 ng/mL) to induce M1 or M2 phenotypes. Cells were then treated with 30 µg/mL ITA-NPs of different molecular weights, for 24 hours as depicted **(a)**. The supernatants for M0 **(b)**, M1 **(c)**, and M2 **(d)** macrophages were evaluated for IL-6, TNF-α, and MCP-1. Bar graphs are presented as mean MFI values ± SD, where *n* = 3 for each condition. Statistical differences were determined by one-way ANOVA with Fisher's LSD test, with significant p values listed above the compared groups. Panel **a** created with Biorender.com

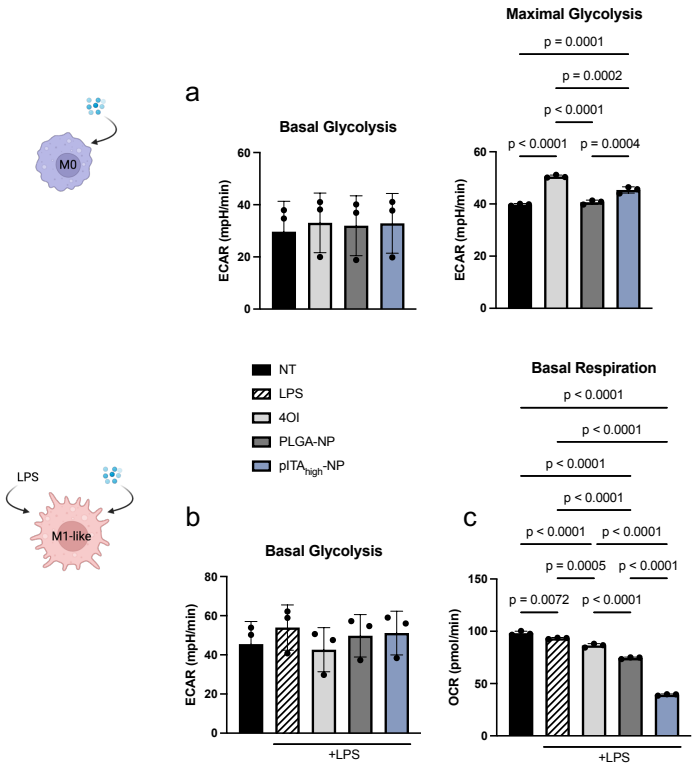

Supplementary Figure 12. NP induced metabolism alterations. Primary macrophages were stimulated with 100 ng/mL LPS overnight to induce an M1 phenotype. Cells were treated for 24 hours with 125 μM 4OI, or 30 μg/mL NPs, then analyzed for using a Seahorse Extracellular Flux XF-96 analyzer. In M0 macrophages, the basal and maximal glycolysis was assessed **(a)** and in M1 macrophages, both the basal glycolysis **(b)** and respiration **(c)** were determined. Bar graphs are presented as mean values ± SD, where *n* = 3 for each condition. Statistical differences were determined by one-way ANOVA with Tukey's multiple comparisons test, with significant p values listed above the compared groups.

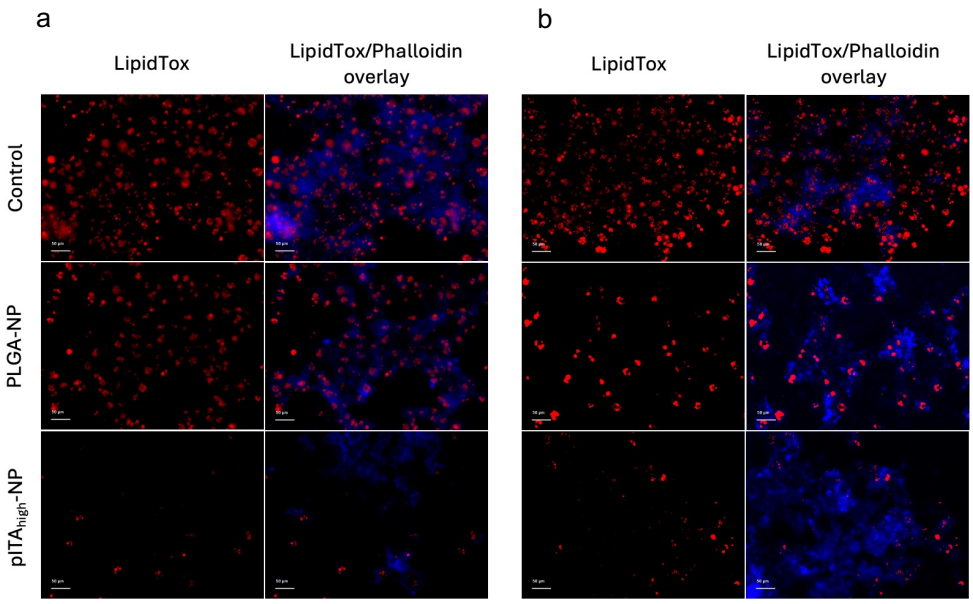

Supplementary Figure 13. pITA$_{high}$-NP treatment decreases lipid accumulation over time. M1 Macrophages were treated with 20 µg/mL NPs on the top layer of a transwell plate, to evaluate the cross talk to mature 3T3-L1 adipocytes seeded on the bottom. At 24 **(a)** and 48 **(b)** hours, adipocytes were stained with LipidTox (red) and Phalloidin (blue) to visualize the decrease in lipid droplets.

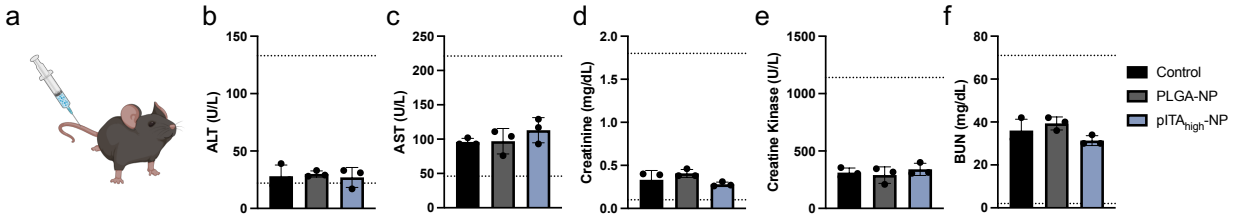

Supplementary Figure 14. pITA$_{high}$-NP is non-toxic. a. Naïve C57BL/6 mice (*n* = 3 per group) were treated intravenously with 200 µL (10 mg/mL NP concentration) of saline, PLGA-NP, or pITA$_{high}$-NP for 24 hours. Plasma was collected and analyzed for ALT (**b**), AST (**c**), creatinine (**d**), creatine kinase (**e**), and BUN (**f**). Dashed lines represent healthy ranges.

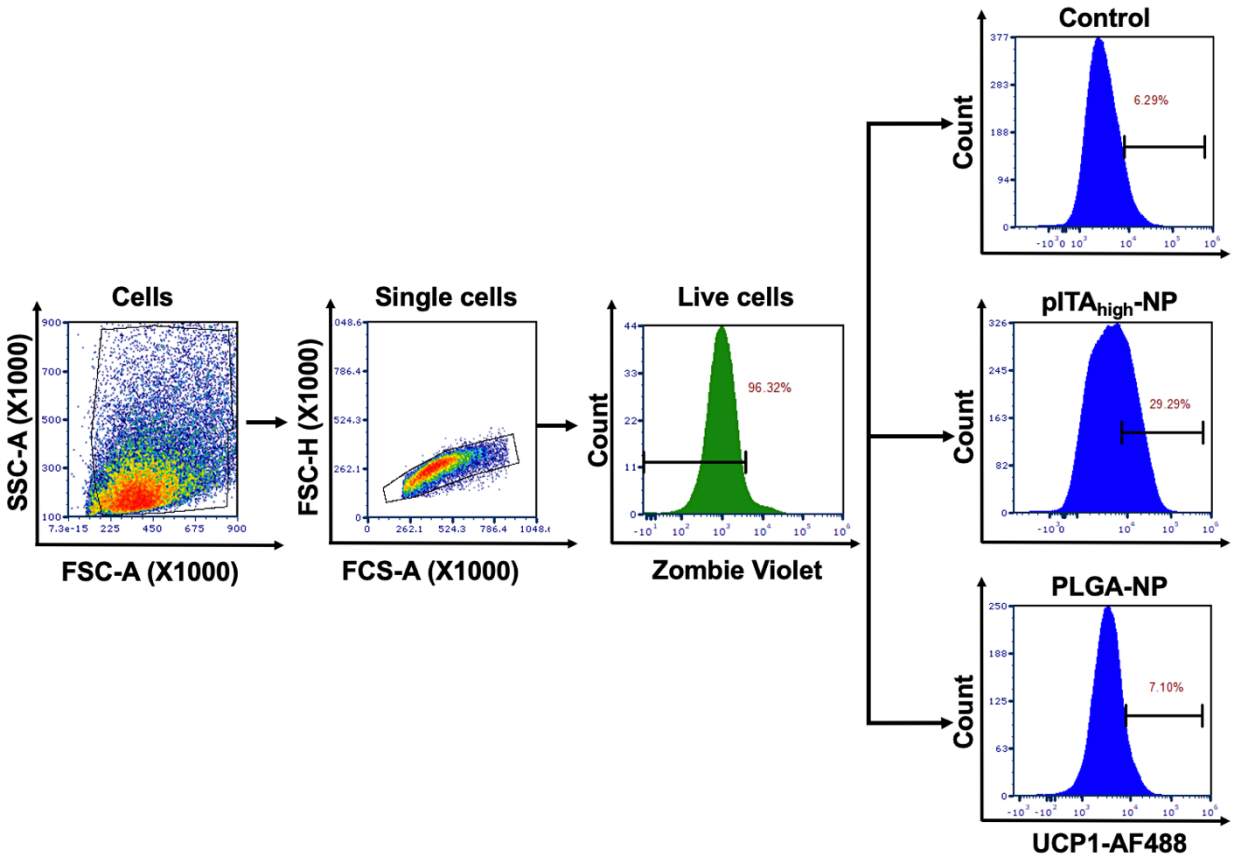

Supplementary Figure 15. Representative gating strategy for *in vivo* studies. Adipose tissue was isolated and processed for analysis by flow cytometry (ZE5, BioRad). Adipocytes were gated as shown. The percent positive UCP1 cells were used for data presentation.

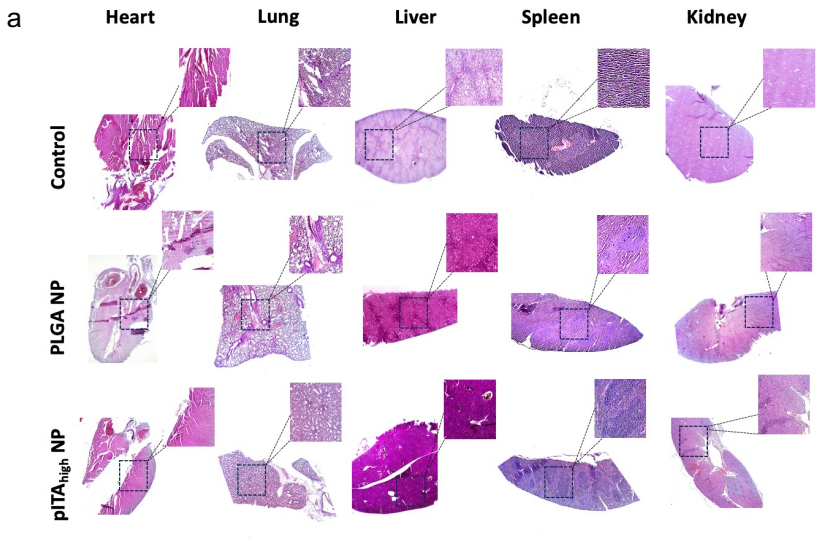

Supplementary Figure 16. Systemic effects of pITA$_{high}$-NPs in HFD mice. a. At day 30, the heart, lungs, liver, spleen, and kidneys were collected and H&E stained to assess toxicity and morphology changes in the tissues.

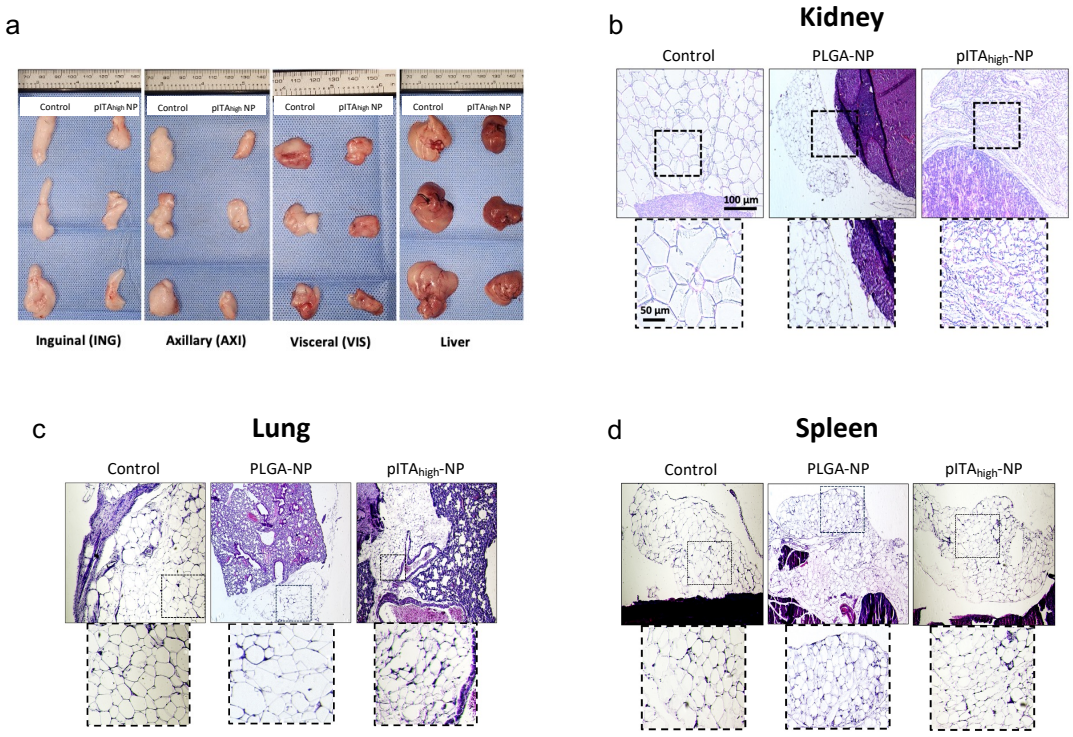

Supplementary Figure 17. Local transformation of adipose tissue. At day 30 of the study, the inguinal, axillary, visceral fat pads and livers were collected and imaged **(a)**. Additional organs were collected, fixed, and sectioned for H&E staining to observe changes in the fat tissue surrounding the kidneys **(b)**, lungs **(c)**, and spleen **(d)**.

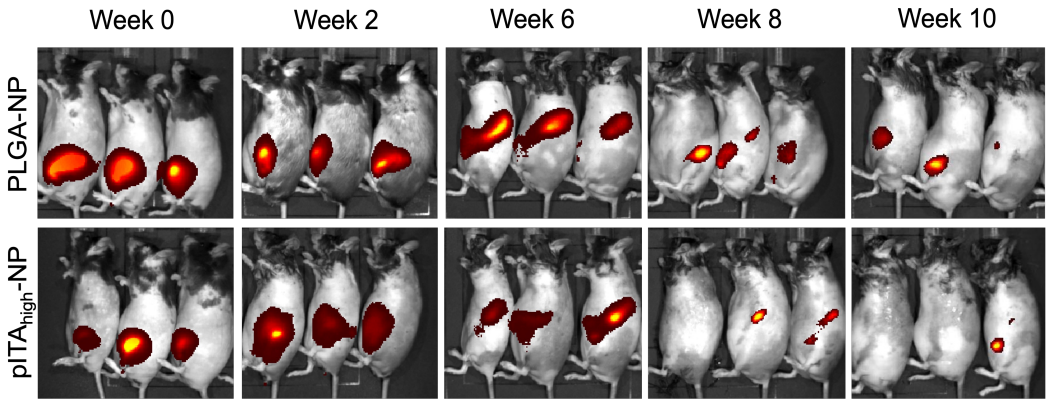

Supplementary Figure 18. Biodistribution profile of NPs in HFD mice. Mice were anesthetized with 2% isoflurane and received an intraperitoneal injection of Cy5.5-labeled NPs at a dose of 16 mg/kg body weight, equivalent to one ING injection. Whole-body fluorescence imaging was performed at 0, 2, 6, 8, and 10 weeks post-injection, using a 1 s exposure time.

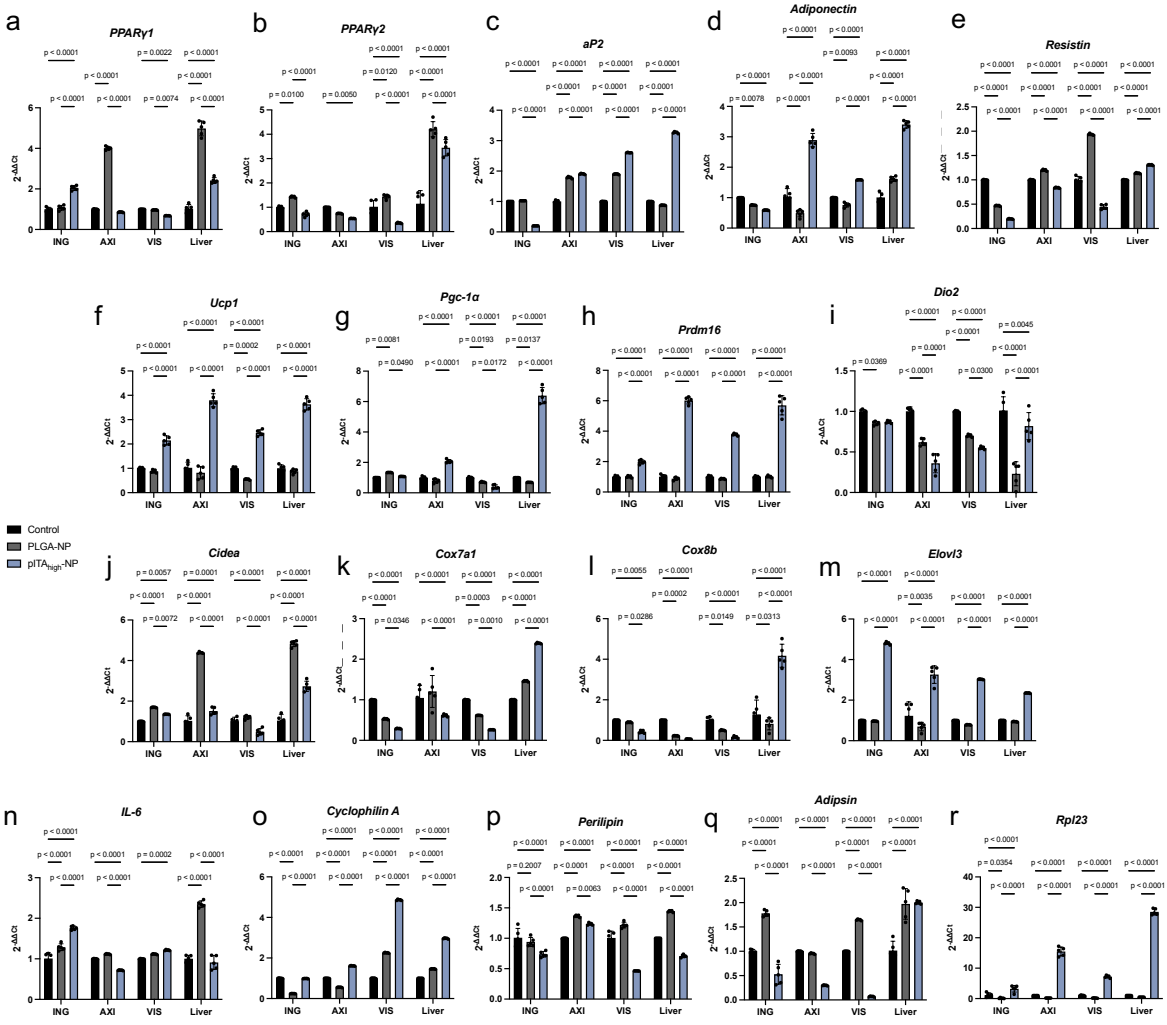

Supplementary Figure 19. pITA$_{high}$-NPs regulate transcription of key genes. RNA was extracted from the inguinal (ING), axillary (AXI), visceral (VIS) fat pads and livers and analyzed via qPCR to assess changes between the HFD control mice and the PLGA-NP and pITA$_{high}$-NP mice. Selected genes evaluated adipogenesis **(a-e)**, thermogenesis **(f-m)**, inflammation **(n-o)**, and lipid droplet and energy storage **(p-r)**. Bar graphs are representing $2^{-\Delta\Delta Ct}$ values, *n* = 5 mice. Error reported as ± SEM. Statistical differences were determined by two-way ANOVA with Tukey's multiple comparisons test, with significant p values listed above the compared groups.

Table 1. Primer sequences were employed for in vitro qRT-PCR analysis.

Gene		Sequences
IL-10	Forward	CGG GAA GAC AAT AAC TGC ACC C
	Reverse	CGG TTA GCA GTA TGT TGT CCA GC
TGF1	Forward	TGA TAC GCC TGA GTG GCT GTC T
	Reverse	CAC AAG AGC AGT GAG CGC TGA A
STAT6	Forward	ACG ACA ACA GCC TCA GTG TGG A
	Reverse	CAG GAC ACC ATC AAA CCA CTG C
CPT1A	Forward	GGC ATA AAC GCA GAG CAT TCC TG
	Reverse	CAG TGT CCA TCC TCT GAG TAG C
Ym1	Forward	TAC TCA CTT CCA CAG GAG CAG G
	Reverse	CTC CAG TGT AGC CAT CCT TAG G
Arg1	Forward	CAT TGG CTT GCG AGA CGT AGA C
	Reverse	GCT GAA GGT CTC TTC CAT CAC C
Mrc1	Forward	GTT CAC CTG GAG TGA TGG TTC TC
	Reverse	AGG ACA TGC CAG GGT CAC CTT T
PParg	Forward	GTA CTG TCG GTT TCA GAA GTG CC
	Reverse	ATC TCC GCC AAC AGC TTC TCC T
Nos2	Forward	GAG ACA GGG AAG TCT GAA GCA C
	Reverse	CCA GCA GTA GTT GCT CCT CTT C
TNFa	Forward	GGT GCC TAT GTC TCA GCC TCT T
	Reverse	GCC ATA GAA CTG ATG AGA GGG AG
IL-6	Forward	TAC CAC TTC ACA AGT CGG AGG C
	Reverse	CTG CAA GTG CAT CAT CGT TGT TC
IL-12	Forward	TTG AAC TGG CGT TGG AAG CAC G
	Reverse	CCA CCT GTG AGT TCT TCA AAG GC
GAPDH	Forward	CAT CAC TGC CAC CCA GAA GAC TG
	Reverse	ATG CCA GTG AGC TTC CCG TTC AG
BActin	Forward	CAT TGC TGA CAG GAT GCA GAA GG
	Reverse	TGC TGG AAG GTG GAC AGT GAG G
NRF2	Forward	CAG CAT AGA GCA GGA CAT GGA G
	Reverse	GGA CAG CGG TAG TAT CAG CCA G
HIF-1α	Forward	CTT GAC AAG CTA GCC GGA GG
	Reverse	GCG CGG AGA AAG AGA CAA GT
NRPL3	Forward	CTC GTC ACC ATG GGT TCT GGT
	Reverse	CGT ATG TCC TGA GCC ATG GAA G

Supplementary Table 1. *In vitro* PCR Primers used in Figure 2.

Table 2. Primer sequences were employed for in vivo qRT-PCR analysis.

Gene		Sequences
Adipsin	Forward	CAT GCT CGG CCC TAC ATG G
	Reverse	CAC AGA GTC GTC ATC CGT CAC
Adiponectin	Forward	GCA CTG GCA AGT TCT ACT GCA A
	Reverse	GTA GGT GAA GAG AAC GGC CTT GT
aP2	Forward	ACA CCG AGA TTT CCT TCA AAC TG
	Reverse	CCA TCT AGG GTT ATG ATG CTC TTC A
Cidea	Forward	TGC TCT TCT GTA TCG CCC AGT
	Reverse	GCC GTG TTA AGG AAT CTG CTG
Cox7a1	Forward	CAG CGT CAT GGT CAG TCT GT
	Reverse	AGA AAA CCG TGT GGC AGA GA
Cox8b	Forward	GAA CCA TGA AGC CAA CGA CT
	Reverse	GCG AAG TTC ACA GTG GTT CC
Cyclophilin A	Forward	TAT CTG CAC TGC CAA GAC TGA GTG
	Reverse	CTT CTT GCT GGT CTT GCC ATT CC
Dio2	Forward	AGA GTG GAG GCG CAT GCT
	Reverse	GGC ATC TAG GAG GAA GCT GTT C
Elovl3	Forward	CCA ACA ACG ATG AGC AAC AG
	Reverse	CGG GTT AAA AAT GGA CCT GA
IL-6	Forward	TTC CAT CCA GTT GCC TTC TT
	Reverse	ATT TCC ACG ATT TCC CAG AG
Perilipin	Forward	GGC CTG GAC GAC AAA ACC
	Reverse	CAG GAT GGG CTC CAT GAC
Pgc-1α	Forward	CCC TGC CAT TGT TAA GAC C
	Reverse	TGC TGC TGT TCC TGT TTT C
PPARγ1	Forward	AGA AGC GGT GAA CCA CTG AT
	Reverse	GAA TGC GAG TGG TCT TCC AT
PPARγ2	Forward	TCT GGG AGA TTC TCC TGT TGA
	Reverse	GGT GGG CCA GAA TGG CAT CT
Prdm16	Forward	TGG CCT TCA TCA CCT CTC TGA A
	Reverse	TTT CTG ATC CAC GGC TCC TGT GA
Resistin	Forward	AAG AAC CTT TCA TTT CCC CTC CT
	Reverse	GTC CAG CAA TTT AAG CCA ATG TT
Rpl23	Forward	TGT CGA ATT ACC ACT GCT GG
	Reverse	CTG TGA AGG GAA TCA AGG GA
Ucp1	Forward	ATG TAC ACC AAG GAA GGA C
	Reverse	GGT ACA ATC CAC TGT CTG TC

Supplementary Table 2. *In vivo* PCR Primers used in Figure 5.